

## Sodium Variable Conductance Heat Pipe with Carbon-Carbon Radiator for Radioisotope Stirling Systems

Calin Tarau and William G. Anderson

Advanced Cooling Technologies, Inc.

1046 New Holland Ave.

Lancaster, PA 17601 U.S.A.

717-295-6066, [Calin.Tarau@1-act.com](mailto:Calin.Tarau@1-act.com), 717-295-6104, [Bill.Anderson@1-act.com](mailto:Bill.Anderson@1-act.com)

### ABSTRACT

In a Stirling radioisotope system, heat must continually be removed from the General Purpose Heat Source (GPHS) modules to maintain the modules and surrounding insulation at acceptable temperatures. The Stirling converter normally provides this cooling. An alkali-metal Variable Conductance Heat Pipe (VCHP) has been developed to provide back-up cooling, allowing multiple stops and restarts of the Stirling converter. Unlike standard VCHPs which maintain a relatively constant temperature, this VCHP has two different heat rejection surfaces. During normal operation, heat is transferred to the Stirling converter heater head. When the Stirling converter is stopped, the VCHP temperature increases by 30°C, and the gas front is pushed back, allowing the heat from the GPHS to be rejected to the Cold Side Adapter Flange (CSAF) using a low-mass, carbon-carbon radiator. The 880°C temperature when the Stirling converter is stopped is high enough to avoid risking standard ASRG operation, but low enough to save most of the heater head life. The Haynes 230/sodium VCHP was successfully tested with a turn-on  $\Delta T$  of 30°C in three orientations: horizontal, gravity-aided, and against gravity.

**KEY WORDS:** Variable Conductance Heat Pipe, Carbon-Carbon Radiator, Radioisotope Stirling System, Advanced Stirling Radioisotope Generator

### 1. INTRODUCTION

In the Advanced Stirling Radioisotope Generator (ASRG), two General Purpose Heat Source (GPHS) modules supply heat to dual Stirling converters (Stirling engine with an integrated linear alternator) (Chan, Wood, and Schreiber, 2007). This heat is used to generate electric power, while the waste heat is radiated to space. The maximum allowable GPHS module operating temperature is set by the iridium cladding around the fuel. The GPHS module is designed so that it will not release radioisotopes, even under such postulated events as a launch vehicle explosion, or reentry through the earth's atmosphere. However, if the iridium cladding was to overheat, grain boundary growth could weaken the cladding, possibly allowing radioisotopes to be released during an accident. Once the GPHS is installed in the radioisotope Stirling system, it must be continually cooled. Normally, the Stirling converter removes the heat, keeping the GPHS modules cool. There are three basic times when it may be desirable to stop and restart the Stirling converter:

1. During installation of the GPHS
2. During some missions when taking scientific measurements to minimize electromagnetic interference and vibration
3. Any unexpected stoppage of the converter during operation on the ground or during a mission.

In the current system design, the insulation spoils (partially melts) if the converter stops, to protect the GPHS from overheating. A VCHP was developed to allow converter operation to be restarted on a planned converter stoppage and potentially allow for converter restart on any unexpected stoppage, depending on the reason for the stoppage. It would also save replacing the insulation after such an event during ground testing.

In a normal VCHP, the Non-Condensable Gas (NCG) front blankets a portion of the condenser surface. As the temperature increases slightly, the increased vapor pressure compresses the NCG, exposing more of the condenser surface. The NCG reservoir is sized to maintain the evaporator

temperature near a nominal temperature as the power is increased or decreased.

In contrast, the current VCHP has two different heat rejection surfaces. One surface supplies heat to the

Stirling convertor during normal operation, while the other is used to dump the heat from the GPHS when the Stirling convertor is off.

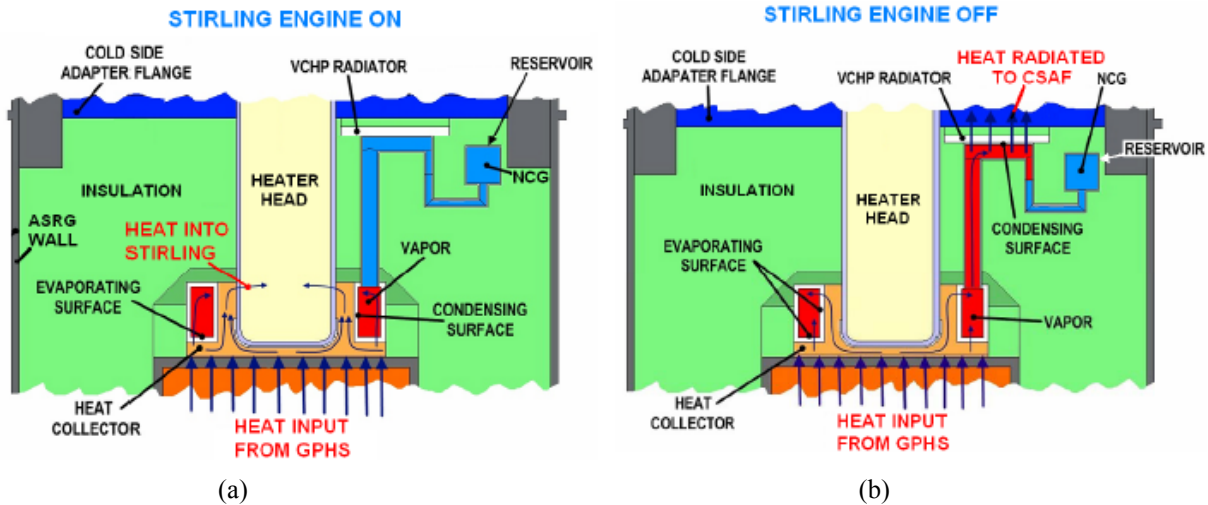


Figure 1. a) VCHP delivers heat to the heater head when the Stirling engine is working. b) VCHP dumps heat to the radiator when the Stirling engine is stopped.

The schematics in Fig. 1 show the basic concept of the VCHP integrated with a Stirling convertor. A GPHS module supplies heat to the heat collector which, in turn, wraps around the hot end of the Stirling convertor’s heater head, so the normal heat flow path is GPHS – heat collector – heater head. The annular evaporator of the VCHP wraps around the heat collector so, during normal operation, vapor is approximately at the heater head’s temperature. The non-condensable gas (NCG) charge in the system is sized so the radiator is blocked during normal operation (see Fig. 1(a)). When the Stirling engine is

stopped, the temperature of the entire system starts to increase. Since the system is saturated, the working fluid vapor pressure increases as the temperature increases. This compresses the NCG. As shown in Fig. 1b, this opens up the radiator. Once the radiator is fully open, all of the heat is dumped to the radiator, and the temperature stabilizes. Once the Stirling engine starts operating again, the vapor temperature and pressure start to drop. The non-condensable gas blankets the radiator, and the system returns back to the normal state (Fig. 1(a)).

Table 1. VCHP Design Requirements.

GPHS Power (W)	250
GPHS Power to the Stirling Engine (W)	225
Heater Head Temperature (°C)	850
Heater Head Material	Mar-M 247
Conduction Losses down the Heater Head Wall (W)	6.5
Heat Collector Material (Baseline)	Nickel 201
Potential Reservoir Location	Embedded in the Insulation
Heat Pipe Material	Haynes 230
Heat Pipe Wick	304 SS Screen
Heat Pipe Working Fluid	Sodium
VCHP Temperature when Stirling is OFF (°C)	880

The Advanced Stirling Radioisotope Generator (ASRG) (Chan, Wood, and Schreiber, 2007) was selected as the baseline Stirling system design. The system consists of two Advanced Stirling Convertors (ASCs), mounted back to back to minimize vibration. Heat to each ASC is supplied by one GPHS module. A cold-side adapter flange, shown in Fig. 1 is used to conduct the waste heat from the Stirling engine cold side to the ASRG housing. This is fabricated from copper, and serves as a structural member. As shown in Fig. 1, when the Stirling convertor is turned off, then the radiator dumps all of the heat from the GPHS to the Cold Side Adapter Flange (CSAF).

A summary of the design requirements is presented in Table 1. The heater head hot-end temperature was 850°C for this program, compared to the current ASRG engineering unit temperature of 650°C.

## 2. VCHP DESIGN

A schematic of the VCHP prototype is shown in Figures 2 and 3. Heat passes through the heat collector and into the annular heat pipe evaporator, which in the real system would surround the Stirling convertor heater head. During normal operation, the NCG blocks the remainder of the VCHP. Heat is transferred from the bottom of the evaporator to the inner wall, where it provides energy to the Stirling convertor.

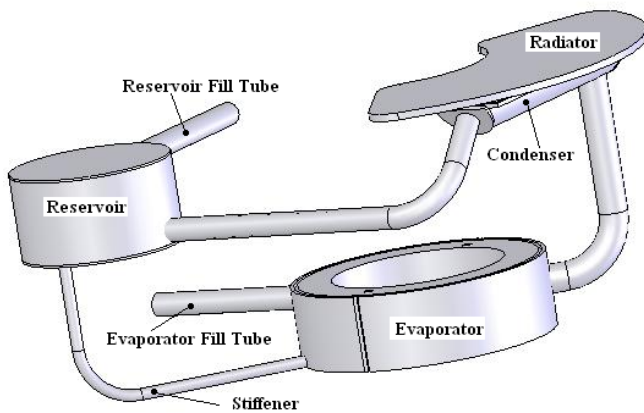


Figure 2. VCHP prototype design.

A tube runs from the annular evaporator to a secondary condenser and radiator. A second tube then runs from the condenser to the NCG reservoir. When the Stirling engine stops, heat is no longer removed from the inner evaporator. The temperature and pressure inside the VCHP increase, driving the NCG front past the condenser and radiator. Heat is

removed by radiation to the CSAF, until Stirling engine is started up again. As the temperature drops, the NCG front moves close to the evaporator again, cutting off the secondary radiator.

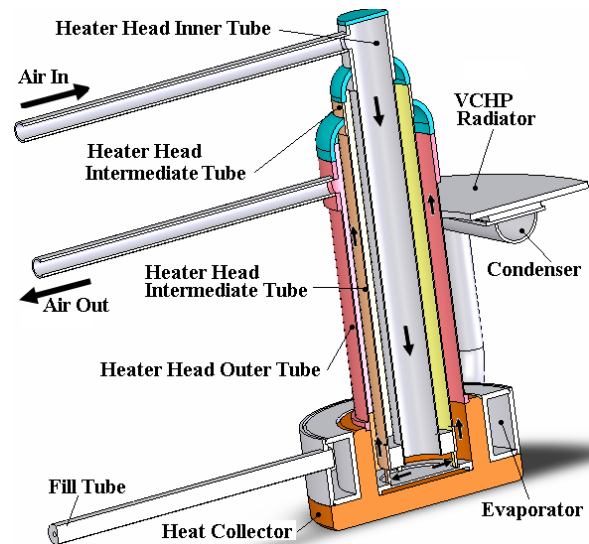


Figure 3. VCHP radiator and heater head simulator.

A cut-away of the VCHP with the heater head simulator is shown in Fig. 3. In a Stirling convertor, heat is removed by the unsteady flow of gas through the heater head. For these experiments, the heater head is simulated by an annular tube assembly where compressed air enters through the inner tube and exits through the annular space, removing the heat by convection from the heat collector - heater head interface region. The air flow rate is monitored by a Pitot tube, while inlet and outlet temperatures are monitored by intrusive thermocouples.

### 2.1 Reservoir Design

The reservoir is located under the CSAF, in the insulation surrounding the Stirling convertor. The initial concept was to locate the reservoir so that its temperature would be relatively stable when the convertor was turned on and off. After numerous CFD iterations to determine a reservoir location with a small  $\Delta T$ , it was determined that the minimum change would be 300-400 K. Since this change in temperature is unacceptable (the reservoir size would increase unrealistically), the system design was modified to cool the reservoir by radiation to the CSAF.

If both the VCHP geometry (except the reservoir size) and reservoir steady state cold temperature

(ASC is ON) are fixed, then the reservoir size becomes a function of the following:

- Steady state hot reservoir temperature (ASC is OFF)
- Temperature difference ( $\Delta T$ ) necessary to turn the VCHP ON.

Figure 4 shows the required reservoir volume as a function of these two parameters for a certain fixed geometry and reservoir cold temperature (in this case the cold reservoir temperature is the origin, 450 K). It is clearly shown that for each selected  $\Delta T$ , the reservoir size increases very abruptly beyond a certain hot reservoir temperature. For example, with a 30°C  $\Delta T$ , the reservoir volume exceeds reasonable values (20-40 cm<sup>3</sup>) very abruptly when the hot reservoir temperature is ~570 K.

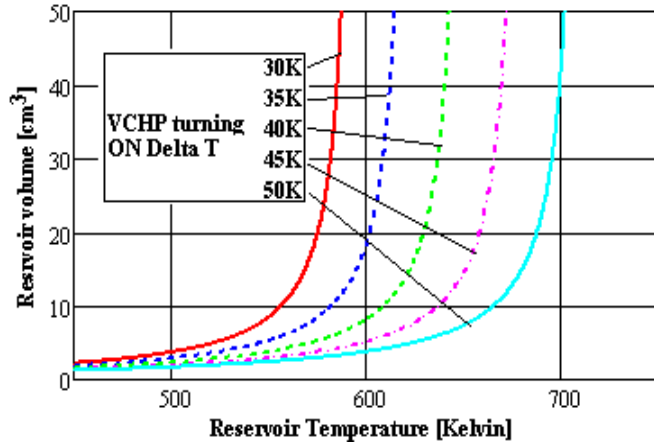


Figure 4. Reservoir size as a function the turning ON  $\Delta T$  and its hot temperature when the cold temp. is fixed at 450 K.

If we chose 17 cm<sup>3</sup> as the upper limit of a reasonable reservoir volume, then, for a 30 K turn-on  $\Delta T$ , the maximum hot reservoir temperature we can have is 571K. The only possibility that allows a good design for higher hot reservoir temperature values is to increase the VCHP turn-on  $\Delta T$ , with possible significant impact on heater head life. As an example, for the same 17 cm<sup>3</sup> reservoir volume but with a 50 K VCHP turning-ON  $\Delta T$ , the hot reservoir temperature will be 681 K. Higher  $\Delta T$ s are undesirable, since it may require lowering the nominal operating temperature to avoid creep problems over the life of the system.

It was determined (but not shown here) that the VCHP tubing size before and after condenser does

not influence the reservoir volume significantly. The reservoir volume was calculated for four different ratios of the reservoir volume to the adiabatic/condenser volumes,  $V_{og}/(V_{cg}+V_{cdg})$ , where:

- $V_{og}$ , is the VCHP volume between the end of the condenser and the entrance of the reservoir
- $V_{cg} + V_{cdg}$  is the VCHP volume between the evaporator and the end of the condenser.

A significant geometry change (9 times higher volume ratio) has a small impact on the allowable hot reservoir temperature, increasing it by only 12 K. This analysis confirmed that the VCHP must be designed under the following restrictions:

- Cold reservoir temperature should be at least 450 K (the objective is to increase it).
- A reasonable reservoir size would be around 17 cm<sup>3</sup> (the objective is to keep it low).
- VCHP turning-ON temperature difference should be around the original 30K (the objective is to keep it low).
- Hot reservoir temperature should be around 570-680K (the objective is to decrease it).
- Since the geometry (volume ratio) impact on the above parameters is weak, it is convenient to keep the current pipe length and choose the closest standard and off-the-shelf tube diameters available for Haynes 230.
- Finding the proper location of the reservoir and solutions to keep the hot reservoir temperature in the above range became mandatory.

The solution of the reservoir temperature problem was solved by creating artificial heat leaks from the reservoir to CSAF by radiation through an aperture in the insulation. These heat leaks are in the order of 1W.

## 2.2 Prototype VCHP

The prototype VCHP is shown in Fig. 5. The VCHP fabrication material is Haynes 230 because of both its compatibility with sodium based on long duration life tests by NASA Glenn (Rosenfeld et al. 2004) and its low creep rate at 850°C. At the bottom of the annular evaporator is the heat collector that receives heat from the GHPS simulator. The heater head simulator, which removes the heat during normal

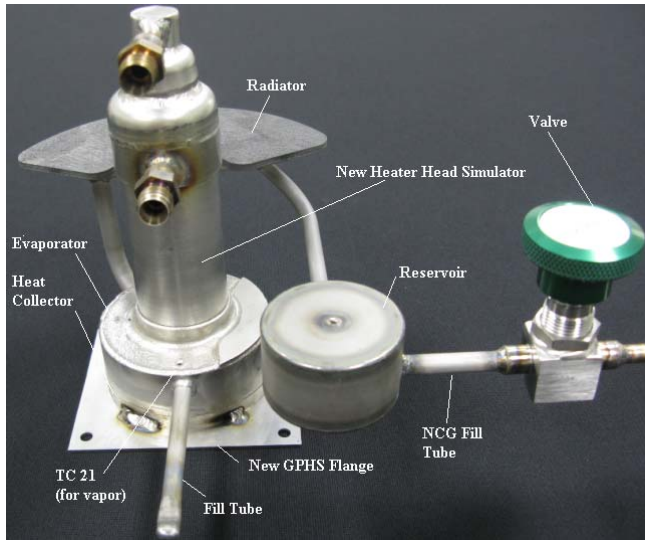


Figure 5. Prototype VCHP.

operation (ASC “ON”) is brazed to the upper/inner side of the evaporator. The carbon-carbon radiator is shown behind the heater head simulator. It is shaped to fit around the Stirling converter (or simulator). Finally, the NCG reservoir is located at the front of Fig. 5. The radiator mass is significantly reduced by using a carbon-carbon radiator, due to both the lower density and higher thermal conductivity. The radiator, shown in Fig. 6, was fabricated by Allcomp, Inc with the following components:

- Carbon-carbon (C-C) radiator panel (2 mm thick)
- POCO foam to accommodate the C.T.E. mismatch between the Haynes and the carbon-carbon
- Condenser back plate (Haynes 230)
- Condenser shell (Haynes 230)
- VCHP evaporator-condenser connecting tube (Haynes 230)
- VCHP condenser-reservoir connecting tube (Haynes 230)

Details of the radiator design and fabrication can be found in Tarau et al. (2010).

### 3. EXPERIMENTAL SETUP

The testing setup is designed to simulate the VCHP behavior with a simulated ASRG and GPHS; see Figure 7. Two of the four copper walls were removed in this picture. Prior to testing, the empty space inside the copper box was filled with Micro-Therm insulation. Four adjustable legs are attached to

the setup to allow testing in different orientations inside the vacuum chamber.

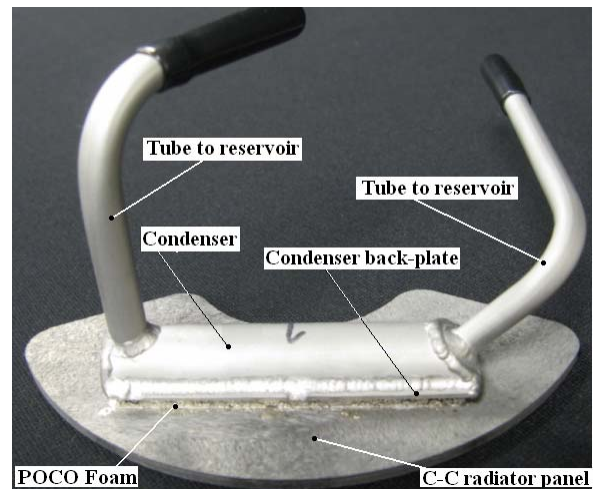


Figure 6. Condenser – C-C radiator assembly.

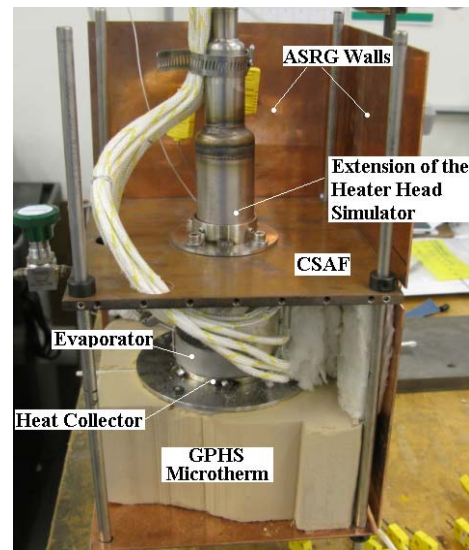


Figure 7. Experimental test setup for the VCHP prototype.

Figure 8 shows the locations of the thermocouples used to measure the temperature distribution along the VCHP. Thermocouples from 1 to 20 were spot welded to the pipe. The remainder were inserted into thermo-wells. Thermocouple 36 measures the NCG temperature in the reservoir while thermocouples 21 and 23 (not shown in Fig. 8) measure the vapor temperature in the evaporator. Thermocouples 24 and 27 (24 is not shown in the figure) measure the heat collector wall temperature

under the vapor space. These thermocouples can be seen in Figures 9 through 11 as components of the entire VCHP temperature profile.

The remainder of the thermocouples measure temperatures of the test setup. Those thermocouples, along with other parameters monitored during testing include:

- CSAF temperature
- ASRG wall temperatures
- Vacuum chamber wall temperature
- Heater head simulator temperatures
- Heater temperature
- Air IN and OUT temperatures
- Air velocity (using a Pitot tube)
- Electrical power

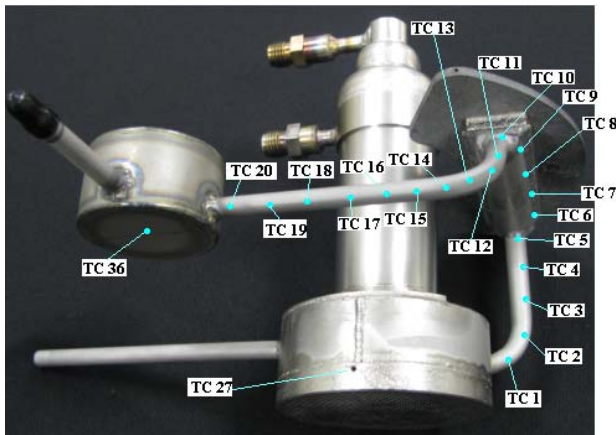


Figure 8. Thermocouple locations along the VCHP.

The average distance between the thermocouple locations along the VCHP is approximately 12 mm. The VCHP was charged with 17 cm<sup>3</sup> of sodium and 4.98 x 10<sup>-4</sup> moles of NCG for the baseline vapor temperature of 850°C.

#### 4. EXPERIMENTAL RESULTS

Since the tests on the previous prototype (similar to the one presented here) were successful in gravity aided, horizontal, and against gravity orientations (Tarau et al., 2010), the final VCHP prototype was tested only gravity aided for the nominal vapor temperature of 850°C. **Error! Reference source not found.** 2, below, summarizes the relevant parameters: electrical power applied to the heater, reservoir temperature, condenser temperature (TC 8), ASRG wall temperature (average), heater temperature and

vacuum chamber wall temperature (average). Numbers 1, 2 and 3 in the second line of **Error! Reference source not found.** 2 refer to the experimental contexts that are described below:

Context 1: Heat Losses: The system is supplied with the minimum electrical power required to maintain a vapor temperature of 850°C under steady state conditions. No cooling is applied during this context and the applied power compensates for all of the heat losses.

Context 2: ASC “ON”, VCHP “OFF”: The heat supplied to the system consists of two components: losses and heat supplied to the ASC (nominally 225 W). In Context 2, cooling is applied to maintain a vapor temperature of 850°C, with the front at the exit of the evaporator (between TC23 and TC1). This context simulates normal operation of the ASRG, before the ASC stoppage and when the VCHP is OFF.

Context 3: ASC “OFF”, VCHP “ON”: The system is continuously supplied with the same total power as in Context 2, however no cooling is applied. This context simulates the system after the ASC is stopped and the VCHP has turned ON, rejecting the heat through the radiator to the CSAF under steady state conditions.

The steady state conditions (reached at the end of each context) will be discussed next, while the transient responses (front motion) will be discussed in the second part of this section. Figure 9 shows the temperature distributions along the VCHP at the ends of the first two contexts. It can be observed from Context 2 that, when cooling is ON (ASC ON), all the temperatures along the VCHP are reasonably close (except the heat collector – TCs 24 and 27) to those corresponding to Context 1 (cooling OFF). This verifies our assumption that the heat losses during Context 1 are equal to those during Context 2. In both contexts, the front is located at the exit of the evaporator at a vapor temperature of 850°C and reservoir temperature of ~160°C. The reservoir temperature as lowered from the ~250°C in Tarau et al. (2010) by redesigning the VCHP to decrease the heat leaks through the VCHP. Of particular importance was using a thinner tube with few screen wraps to decrease the heat leak through the tube connecting the condenser and the reservoir, and increasing the aperture to radiate heat from the reservoir to the CSAF.

Table 2. Relevant parameters during measurements.

Power	Heat Loss	118 W
	VCHP Off	380 W
Reservoir Temp.	Heat Loss	159°C
	VCHP Off	161°C
	VCHP On	246°C
Condenser Temp.	Heat Loss	296°C
	VCHP Off	296°C
ASRG Wall Temp.	Heat Loss	83°C
	VCHP Off	85°C
	VCHP On	166°C
Heater Temp.	Heat Loss	890°C
	VCHP Off	985°C
	VCHP On	1014°C
Chamber Wall Temp	Heat Loss	29°C
	VCHP Off	31°C
	VCHP On	40°C

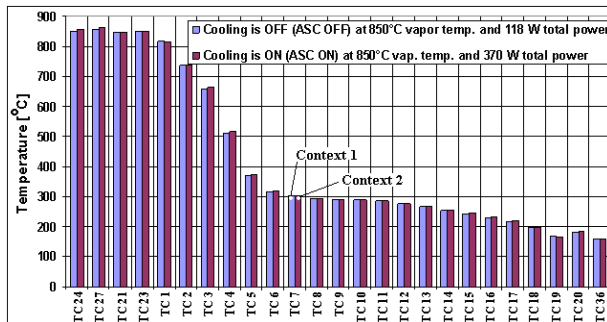


Figure 9. VCHP temperature distributions at steady state for Contexts 1 (heat loss determination) and 2 (Stirling on).

The heat losses during Context 1 are 118 W, while total power (electrical) during Contexts 2 and 3 is 380 W, resulting in a VCHP throughput of approximately 262 W.

Figure 10 shows steady state temperature distributions. The cooling air was initially on (Stirling ON), with the front near the evaporator. The cooling air was shut off (Stirling OFF), activating the VCHP radiator. Under steady state conditions the NCG front settled at the end of the condenser. The

vapor temperature reached an average value of 880°C while the hot reservoir temperature reached 246°C. Finally, the cooling gas was turned back on (Stirling ON). The front settled at the exit of the evaporator (TC1) for a 850°C vapor temperature and 177°C cold reservoir temperature. There is some difference between the two temperature differences with the cooling gas on (Stirling ON), because steady state has not yet been reached.

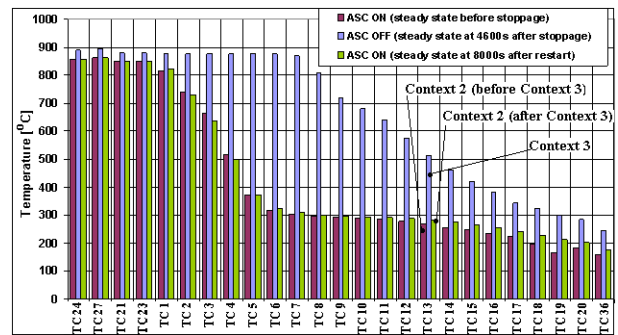
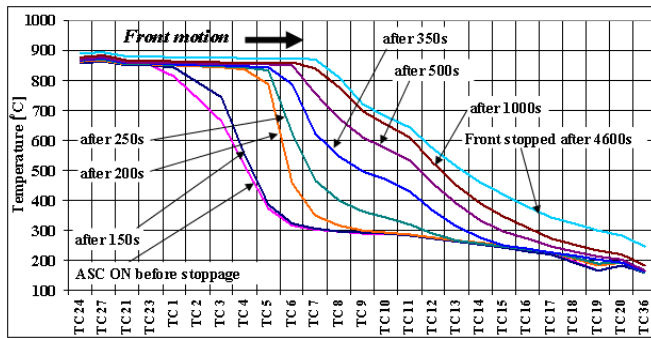


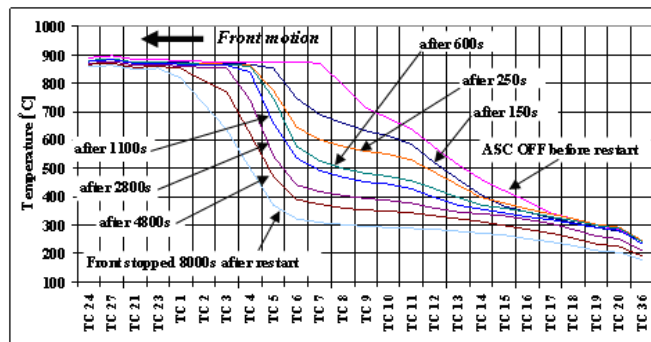
Figure 10. VCHP temperature distributions at steady state for Contexts 2 (Stirling ON) and 3 (Stirling OFF).

The transient VCHP temperature profiles for Contexts 3 (Cooling Gas off, VCHP activated) and 2 (Cooling Gas on, VCHP deactivated) are presented in Figure 11. Figure 11a starts with the lowest temperature profile, where the cooling air is active (ASC ON). The evaporator is at 850°C, and most of the heat is going from the heater, through the annular evaporator, and into the cooling air. The radiator is OFF, with temperatures below 300°C. Once cooling is stopped (ASC OFF), the system starts to heat up, and the NCG gas front moves toward the condenser. As it travels up the condenser, heat is transferred to the wall of the ASRG simulator and then to the ambient (vacuum chamber walls) by radiation.

When cooling is turned on the system gradually cools. The vapor temperature and pressure drop, and the NCG front moves back towards the annular evaporator. As expected, the gas front moves at a faster rate in the beginning and slower toward the end of each of the two sequences, as steady state conditions are approached. It can be observed that the front is slower during the return when the radiator is activated.



a)



b)

Figure 11. VCHP temperature distributions during a) Context 3 (VCHP turns ON) and b) Context 2 (VCHP turns OFF).

## 5. CONCLUSIONS

A sodium VCHP has been developed to provide back-up cooling, allowing multiple stops and restarts of the Stirling convertor. Unlike standard VCHPs which maintain a relatively constant temperature, this VCHP has two different heat rejection surfaces. During normal operation, heat is transferred to one condenser. With no heat removal from the first condenser, the VCHP temperature increases by 30°C, and the gas front is pushed back, allowing the heat to be rejected to a second condenser. While the presented prototype was only tested in the gravity-aided orientation, tests with previous prototypes show that the VCHP can operate in any orientation.

## ACRONYMS

ASC, Advanced Stirling Convertor.  
 ASRG, Advanced Stirling Radioisotope Generator  
 CSAF, Cold Side Adapter Flange  
 C.T.E., Coefficient of Thermal Expansion

GPHS, General Purpose Heat Source  
 NCG, Non Condensable Gas  
 TC, Thermocouple  
 VCHP, Variable Conductance Heat Pipe

## ACKNOWLEDGEMENT

This research was sponsored by NASA Glenn Research Center under Contract No. NNC07QA40P. Any opinions, findings, and conclusions or recommendations expressed in this article are those of the authors and do not necessarily reflect the views of the National Aeronautics and Space Administration. Lanny Thieme is the contract technical monitor. We would like to thank John Hartenstine of Advanced Cooling Technologies, Inc., Jeff Schreiber and Jim Sanzi of NASA Glenn Research Center, Bill Miller, Rogelio Ramirez, and Wei Shih of Allcomp, Inc., and Jaime Reyes, Jack Chan, and Michael Welz of Lockheed Martin Space Systems Company for helpful discussions about the Stirling system and the VCHP. Tim Wagner was the technician for the program.

## REFERENCES

1. Chan, T.S., Wood, J. G. and Schreiber, J. G., "Development of Advanced Stirling Radioisotope Generator for Space Exploration," NASA Glenn Technical Memorandum NASA/TM-2007-214806, 2007.  
<http://gltrs.grc.nasa.gov/reports/2007/TM-2007-214806.pdf>
2. Rosenfeld, J. H., Ernst, D. M., Lindemuth, J. E., Sanzi, J., Geng, S. M., and Zuo, J., "An Overview of Long Duration Sodium Heat Pipe Tests," NASA Glenn Technical Memorandum NASA/TM—2004-212959, 2004.  
<http://gltrs.grc.nasa.gov/citations/all/tm-2004-12959.html>
3. Tarau, C., Anderson, W. G., Miller, W. O., and Ramirez, R., "Sodium VCHP with Carbon-Carbon Radiator for Radioisotope Stirling Systems", Space, Propulsion & Energy Sciences International Forum, Johns Hopkins Applied Physics Laboratory, MD, February 23-25, 2010.
4. C. Tarau, W. G. Anderson, and K. Walker, "Sodium Variable Conductance Heat Pipe for Radioisotope Stirling Systems," 7th International Energy Conversion Engineering Conference, Denver, CO, Aug. 2-5, 2009.